

UDC 528.481

## GEODETIC EVIDENCE FOR POST-SEISMIC DEFORMATIONS FOLLOWING THE 2014 NORTH AEGEAN MW 6.9 EARTHQUAKE

Michail GIANNIOU<sup>id\*</sup>, Panagiotis ARGYRAKIS<sup>id</sup>, Tatiani PRASINO<sup>id</sup>*Department of Surveying and Geoinformatics Engineering, University of West Attica, Athens, Greece*

Received 18 June 2023; accepted 22 November 2023

**Abstract.** The 2014 North Aegean Sea earthquake was a strong (Mw 6.9) event that caused significant crustal deformations. In the present study we investigate the long-term impact of the earthquake on the kinematics of the North Aegean Trough (NAT). For this purpose, we analyzed GPS observations collected from May 2010 to April 2022 at five permanent GPS reference stations. Two of these stations are located close to the epicenter(s) on the Islands of Lemnos and Samothrace. We processed the data using the Precise Point Positioning (PPP) technique. The analysis of the obtained coordinate time-series revealed a post-seismic deformation (PSD) period lasting for more than two years leading to cumulative 2D post-seismic displacement of 22 mm and 27 mm for Samothrace and Lemnos, respectively. The magnitudes of these post-seismic slip vectors correspond to 23% and 49% of the co-seismic vectors at Samothrace and Lemnos, respectively. The long-term analysis showed that after the end of the PSD period the stations are characterized by stable velocities that are noticeably different compared to the velocities prior to the event. We observed a change in the velocity in the order of 2 mm/yr for both Samothrace and Lemnos. It is the first time that PSD and velocity changes have been reported for the 2014 North Aegean Sea earthquake shedding light on the characteristics and the impact of this important earthquake on the kinematics of NAT.

**Keywords:** North Aegean Trough, earthquake, post-seismic deformation, velocity change, GPS, Precise Point Positioning.

### Introduction

The North Anatolian Fault (NAF) is a 1200 km long right-lateral strike-slip fault system that extends from eastern Turkey to the north Aegean (Ergintav et al., 2014; Şengör et al., 2005). NAF has a length of over 1200 km and separates the Anatolian plate from the Eurasian plate (Bulut et al., 2018; Straub et al., 1997). NAF is an active fault of high tectonic significance and has accommodated three major earthquakes since 1999 (Bulut, 2015). It propagates into the Aegean Sea by the 300 km long North Aegean Trough (NAT) (Görgün & Görgün, 2015), a series of sedimentary basins extending from Saros Gulf to the Sporades islands (Konstantinou, 2017). As NAF enters into the Northern Aegean Sea, it splays into two main segments. The most active segment is the northern one, which passes between the islands of Samothrace and Gökçeada, north of Lemnos island and ends up at the Sporades basin (Kiratzi, 2002). The tectonic regime of the area is dominated by the westward motion of Turkey and the southwestward motion of the Aegean microplate by 30 mm/yr w.r.t. Eurasia (Taymaz et al., 1991; Müller et al., 2013). The North Aegean Trough is characterized by strike-slip motions and

NS extension with shear strain reaching 100–150 ns/yr (Chousianitis et al., 2015). The wider area of the North Aegean Trough is one of the most seismically active areas in Greece and is characterized by strong and shallow earthquakes. In the 20th century, several destructive (M6.5–7.5) earthquakes took place in the vicinity of NAT in 1902, 1905, 1931, 1932 (M7.0 Ierissos), 1968 (M7.1 Agios Efstratios) and 1978 (M6.5 Thessaloniki) (Pavlidis & Tranos, 1991).

The latest strong earthquake along NAT stroke on May 24, 2014, between the islands of Samothrace, Lemnos and Gökçeada. The epicenter of this strong (Mw 6.9) event and the area's seismicity from March to October 2014 are depicted in Figure 1. The main damages were caused at the province of Çanakkale and the islands close to the epicenter (Erdik et al., 2014). Saltogianni et al. (2015) used geodetic and seismological observations and indicated that the rupture consisted of two subevents (occurred with a time difference of 14 s) corresponding to two adjacent strike-slip fault segments, one SW of Samothrace and another one SE of the island. The single source seismological analysis corresponds to a right-lateral strike-slip fault at a depth of 11 km, with strike = 75°, dip = 85°

\*Corresponding author. E-mail: [mgianniou@uniwa.gr](mailto:mgianniou@uniwa.gr)

and rake =  $-178^\circ$ . Evangelidis (2015) studied the event by backprojecting strong motion waveforms and reported rupture with supershear velocity ( $\sim 5.5$  km/s). The analysis of GPS observations revealed significant permanent displacements in the wider area of the event reaching  $\sim 5$  cm and  $\sim 10$  cm at the GPS stations in the islands of Lemnos and Samothrace, respectively (Saltogianni et al., 2015). Saltogianni et al. (2016) investigated the dynamic displacements of GPS stations during the event by analyzing 1 Hz GPS data and found a correlation between the kinematic and the static displacements. Sboras et al. (2015) and Bitharis et al. (2016) studied the time-series of the GPS station in Samothrace and concluded that the displacement was not instantaneous during the earthquake, but it was stabilized after approximately two days.

Tiryakioglu et al. (2017) estimated inter-seismic velocities for 12 GPS stations on either side of NAF in Turkey using a period of about 6 years before the 2014 earthquake. They also estimated post-seismic velocities using about 1.5 years of post-earthquake data. The inter-seismic and post-seismic velocities of the stations were found to be very similar. A difference of 2 mm/yr was observed between the inter-seismic velocity of station IPSA and the post-seismic velocity of station IPS1 (the successor of IPSA, relocated 0.55 km from its initial position). No significant post-seismic deformation was detected among the 12 stations investigated (with the exception of one station, which indicated abnormal deformation due to local factors). However, the stations examined by Tiryakioglu et al. are located east of the epicenter and at long distances

between 90 and 250 km from it. Gianniou and Stavropoulou (2016) analyzed data lasting up to one year after the event from a GPS station on the island of Lemnos (which is much closer to the epicenter) and reported a change in the velocity after the 2014 earthquake. Gianniou et al. (2017) analyzed GPS data lasting up to three years after the event and demonstrated that the 2D velocity of the station in Lemnos appeared to be increased by 5 mm/yr.

In order to examine in more detail the implications of the 2014 earthquake on the kinematics of NAT, in this study we systematically searched for post-seismic deformation and changes in the velocities in the area close to the epicenter(s). For this purpose, we used 12-year data collected from May 2010 to April 2022 at five GPS stations. The stations closest to the epicenter are located on the islands of Samothrace and Lemnos at distances of 21 and 47 km from the epicenter, respectively. The availability of 8-year data after the event was proved to be vital for the assessment of the long-term effect of the seismic event on the kinematics of the area.

## 1. Data and methods

### 1.1. Data used

For our research we used data from five permanent GPS reference stations that are located as close as possible to the epicenter of the earthquake. More precisely, we used the following stations: 018B on the island of Samothrace, 089A on the island of Lemnos, 019A near the city of Alexandroupoli, 036A on the island of Thasos and 091A on

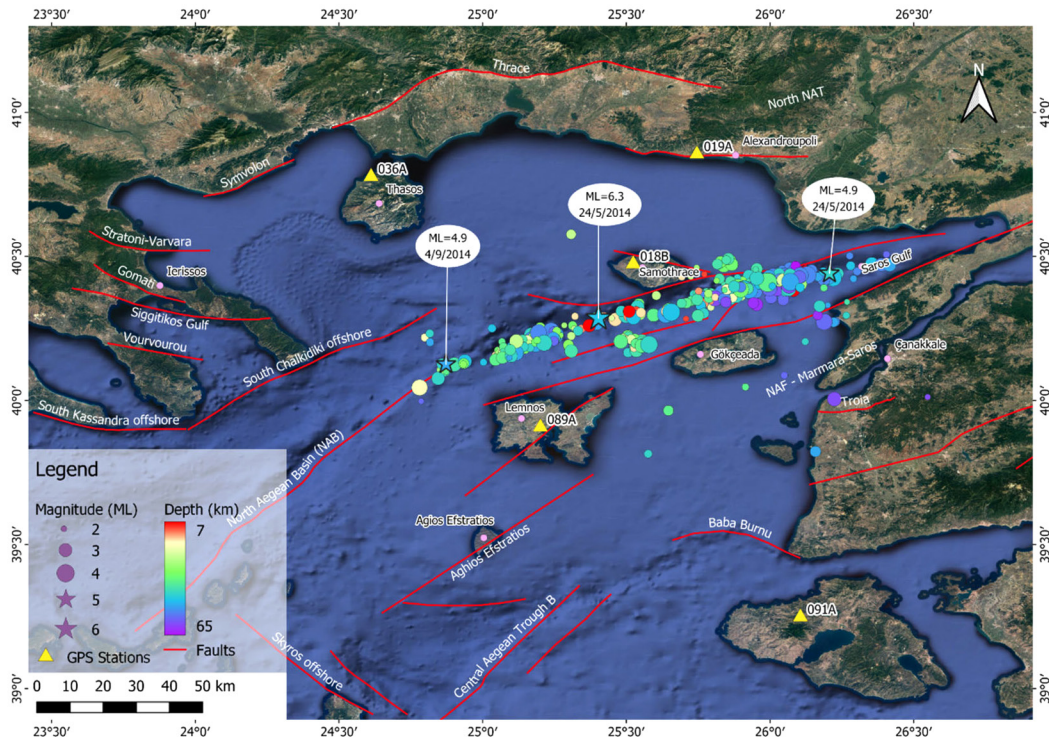


Figure 1. Map of the study area showing the seismicity (ML) along NAT between March and October 2014 (data obtained from the National Observatory of Athens (NOA) database). Stars indicate the three strongest events.

Redlines indicating the main faults are retrieved from the GreDaSS (Caputo et al., 2012) and GEM GAF-DB databases (Styron & Pagani, 2020). Yellow triangles denote the used GPS stations

the island of Lesbos, as shown in Figure 1. These stations belong to the national RTK-network HEPOS (HELlenic POSitioning System) operated by the Hellenic Cadastre (Gianniou, 2008, 2009). All stations were installed in 2007 using equipment of the same kind, i.e. Trimble NetRS dual-frequency GPS geodetic receivers and Trimble Zephyr Geodetic antennae with Trimble hemispherical domes (IGS antenna code “TRM41249.00 TZGD”). The available data sets span from 2010.33 to 2022.33 for 018B & 089A, from 2010.33 to 2020.33 for 019A & 036A and from 2010.33 to 2017.33 for 091A. Taking into consideration that the earthquake occurred at 2014.39, this data span offers four complete years (4×12 months) before the event and up to 8 complete years (8×12 months) after it. This complies with the guidelines issued by EUREF –the IAG (International Association of Geodesy) sub-commission for the European Reference Frame– which foresee the use of at least three years of continuous data for reliable velocity estimation (Legrand et al., 2021). The GPS data were available in daily RINEX files (ver. 2.11) with a sampling interval of 30 s.

## 1.2. Processing scheme

Before proceeding with the data processing all files were scanned to detect incomplete daily files. Such files commonly occur on a station outage’s first and last day. During this pre-processing step 35 incomplete files were detected for station 018B and 39 for station 089A. These incomplete files were excluded from the computations to avoid biased daily solutions. As a result, the total number of daily files that were not used in the processing (missing and incomplete files) was 247 for station 018B and 170 for station 089A. These numbers correspond to 5.6% and 3.8% of the total time-span, for stations 018B and 089A, respectively. The corresponding percentages for stations 019A, 036A and 091A are 18%, 5% and 7%, respectively.

We processed the data using the Precise Point Positioning method (Zumberge et al., 1997; Héroux & Kouba, 2001). Aside from its computational efficiency another advantage of this method is that it makes easier the detection of site-specific issues, like multipath effects, interfering electromagnetic signals etc. (Zumberge et al., 1997). PPP is being successfully used for estimating velocity (Gianniou & Stavropoulou, 2016; Perez et al., 2003) and assessing post-seismic deformations (Vigny et al., 2005; Satirapod et al., 2007). Moreover, under certain conditions PPP is particularly advantageous compared to the relative positioning (baseline solutions). This is e.g., the case when the nearby stations that can be used as base stations in the baseline processing may also be affected by the event being investigated. This is crucial in our study, as the 2014 NAT earthquake caused considerable permanent displacements at a large number of stations around the epicenter up to distances of 130 km (Saltogianni et al., 2015). The GPS data were analyzed utilizing the GipsyX ver. 2.0 software developed by the Jet Propulsion Laboratory (JPL) (<http://gipsy-oasis.jpl.nasa.gov>; Bertiger et al., 2020).

We processed the data at a 30 s rate using an elevation mask of 7°. We decided to use the 30 s rate (instead of the default rate of 300 s) because we found that it slightly improves the results, as will be demonstrated in Section 2. We used final orbits and high-rate clocks issued by JPL and IGS absolute antenna calibration. Tropospheric zenith delays and gradients were estimated considering random walk noise and using the Global Mapping Function (GMF) (Boehm et al., 2006). Ambiguity resolution was enabled. Standard corrections for solid earth tides and pole tides were applied. Moreover, we applied Ocean Tide Loading (OTL) correction. This was vital for our computations, as the GPS stations are located in the north Aegean Sea and are affected by OTL. We used the FES2014B model for computing the amplitudes and phases of the tidal parameters (corrected for the motion of the center of mass of the solid Earth) using the program provided by Scherneck and Bos (2002). The estimated coordinates refer to the International Terrestrial Reference Frame 2014 (ITRF2014) (Altamimi et al., 2016).

The obtained horizontal position estimates were split into two parts: one before and one after the earthquake. The main reason for following this approach was that we wanted to estimate velocities before and after the earthquake, to check for changes in the kinematics of the area caused by the event. As a first step, the time-series of each part were cleaned using a 3-sigma filter. For each part the linear trend was estimated using least squares. The goodness of linear fit was examined using the coefficient of determination  $R^2$  and the WRMS, in order to judge if the linear trend describes adequately the motion of the station. As described in the following section this was the case for all stations for the time period prior to the event. On the contrary, post-seismic deformation was detected after the earthquake, especially for stations 018B and 089A. As known, the position of a station during a post-seismic trajectory can be described as (Altamimi et al., 2016):

$$X_{PSD}(t) = X(t_0) + X'(t - t_0) + \delta X_{PSD}(t), \quad (1)$$

where  $X'$  is the station linear velocity vector and  $\delta X_{PSD}(t)$  is the total sum of the post-seismic deformation (PSD) corrections at epoch  $t$ . This post-seismic motion was assessed using the following logarithmic function (Kremer et al., 2006; Satirapod et al., 2008; Ohta et al., 2008):

$$u(t) = c + a \ln \left( 1 + \frac{t}{\tau_{\log}} \right), \quad (2)$$

where  $t$  denotes the time since the event,  $u(t)$  is the coordinate (East, North),  $c$  is the co-seismic offset,  $a$  is the amplitude associated with the decay, and  $\tau_{\log}$  is the logarithmic decay time.

## 2. Results

As a first preparatory step, we processed the data of station 018B at two different rates (300 s and 30 s) to compare the

Table 1. Statistics of coordinate time-series obtained with different processing rates (30 s and 300 s)

Station	East		North		Up	
	30 s	300 s	30 s	300 s	30 s	300 s
$R^2$	0.977	0.976	0.852	0.834	0.009	0.006
Stdev (mm)	2.85E-03	2.93E-03	3.44E-03	3.66E-03	9.09E-03	9.41E-03

solutions and choose the optimal processing rate for our study. For evaluating the results, a) we computed linear fit to the (un-detrended) East, North, Up time-series and compared the  $R^2$  values and b) we compared the standard deviations of the detrended time-series. Table 1 gives the results for the 3-year long time-series (2011.00–2013.99). As can be seen, the 30 s time-series are characterized by slightly less noise compared to the 300 s ones. Based on these results, we decided to use a processing rate of 30 s throughout our study in order to obtain the highest possible precision.

After processing the data at a 30 s rate and excluding the noisy epochs using the 3-sigma filter mentioned in section 1.2, the cleaned time-series were plotted to obtain

an overall picture of the coordinate evolution. Figures 2–6 give the time-series of East and North for the five stations. The coordinates' shifts caused by the earthquake can clearly be seen at the time of the event (epoch 2014.39) in Figures 2 and 3. Moreover, in Figure 3, a post-seismic deformation can be observed for station 089A in Lemnos, which is more intense for the North coordinates.

Unlike the East and North time-series, the examination of the Up time-series did not reveal any clear displacement in the vertical component, which is in accordance with the nature of the event (strike-slip fault, dip  $\sim 85^\circ$ ). Thus, in our study we analyzed only the horizontal coordinates.

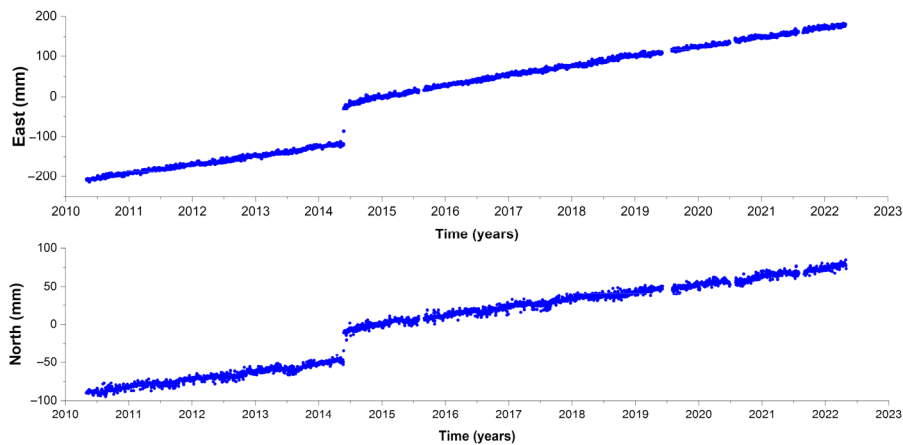


Figure 2. Time-series of local coordinates of station 018B in Samothrace for the complete time period under investigation (2010.33–2022.33)

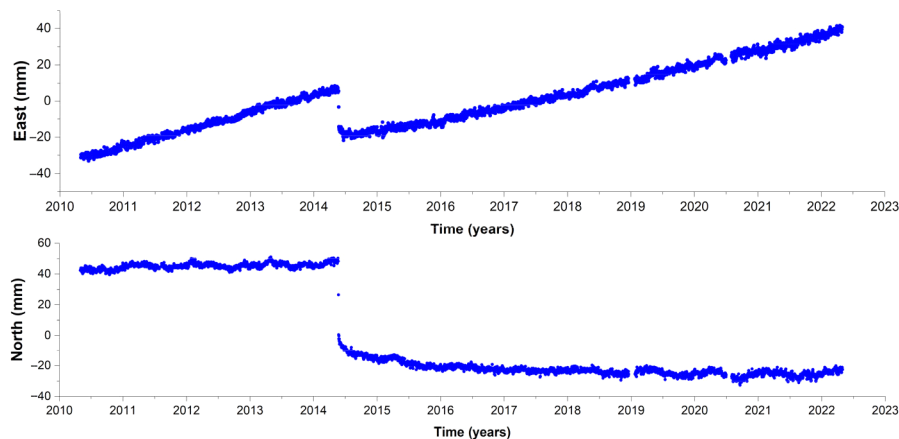


Figure 3. Time-series of local coordinates of station 089A in Lemnos for the complete time period under investigation (2010.33–2022.33)

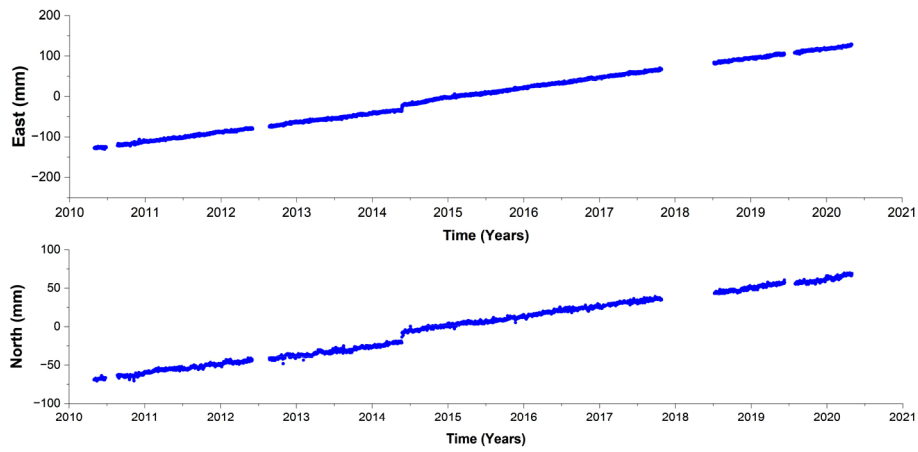


Figure 4. Time-series of local coordinates of station 019A near Alexandroupoli for the complete time period under investigation (2010.33–2020.33)

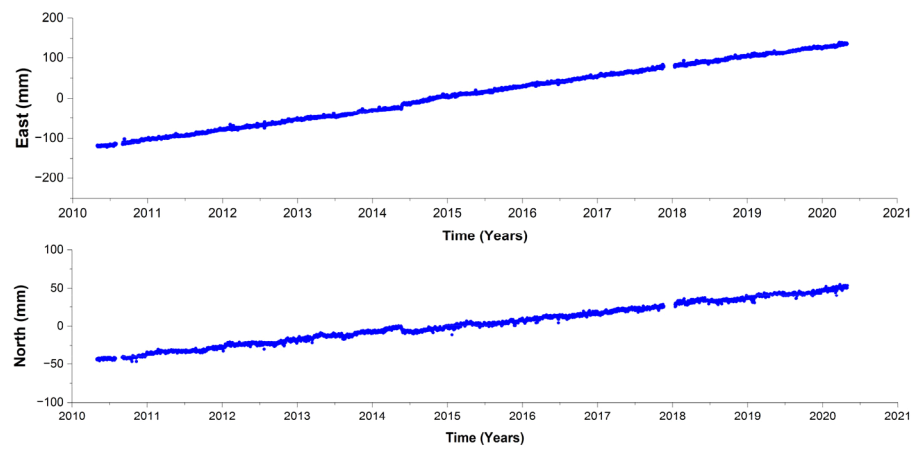


Figure 5. Time-series of local coordinates of station 036A in Thasos for the complete time period under investigation (2010.33–2020.33)

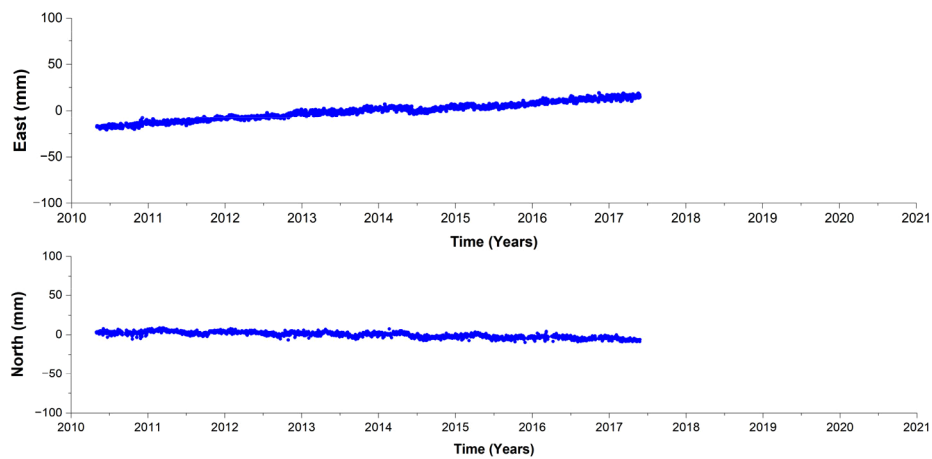


Figure 6. Time-series of local coordinates of station 091A in Lesvos for the available time period (2010.33–2017.33)

## 2.1. Post-seismic deformation

To get a more detailed picture of the post-seismic motion of the stations, the time-series of their coordinates for the time period after the event are plotted separately in the Figures 7–11. As described in detail in Section 2.2, the post-seismic motion of stations 018B and 089A lasted up to 2017 and 2018, respectively; after that, the stations are moving with stable velocities. In order to make the PSD clearer, the upper parts of Figures 7–11 (parts (a) and (b)) are showing the coordinates along with the straight lines representing the stable velocities that are characterizing the stations in the years after the PSD. Looking at Figures 7a and 7b, a small post-seismic motion can be seen for station 018B on Samothrace that lasts about three months and leads to a cumulative deformation of  $\sim 2$  cm and  $\sim 1$  cm, towards East and North, respectively. Looking at Figures 8a and 8b, we see that the PSD at station 089A on Lemnos is more or less in the same order as at station 018B on Samothrace, but it lasts significantly longer.

In order to reveal a more detailed pattern of the PSD, we computed logarithmic functions based on Equations (1) and (2). For solving the non-linear system, we used the Levenberg–Marquardt method (Press et al., 1992). The estimated logarithmic functions along with the detrended coordinates are given in the lower parts of

Figures 7–11 (parts (c) and (d), for the East and North, respectively). The parts (c) and (d) of these Figures are focusing in the first 3 to 4 years after the earthquake, i.e. up to 2017 for the more distant stations (019A, 036A and 091A) and up to 2018 for the closest and mostly affected stations (018B and 089A), as after that time the velocities became stable. The green line in the Figures denotes the seasonal variations (annual and semi-annual signals) that have been estimated for de-noising the observations. It can be seen that the PSD on Samothrace lasts about three years, whereas the PSD on Lemnos lasts longer, i.e. four years. Moreover, the computation of the logarithmic functions allowed the precise estimation of the cumulative PSD for East and North (parameter  $c$  of Equation (2)). The cumulative PSD in Samothrace amounts  $-20$  mm in the EW direction and  $-10$  mm in the SN direction. In Lemnos the cumulative PSD amounts 12 mm in the EW direction and 24 mm in the SN direction. Examining Figures 9–10 it can be seen that smaller post-seismic deformations in the order of 5 mm took place also at stations 019A and 036A. However, they affected only the East coordinate. From Figure 11 it comes out that station 091A on Lesvos was not affected at all by PSD. The cumulative PSD values for all stations are summarized, together with the 2D displacements, in Table 2. All the above-mentioned post-seismic

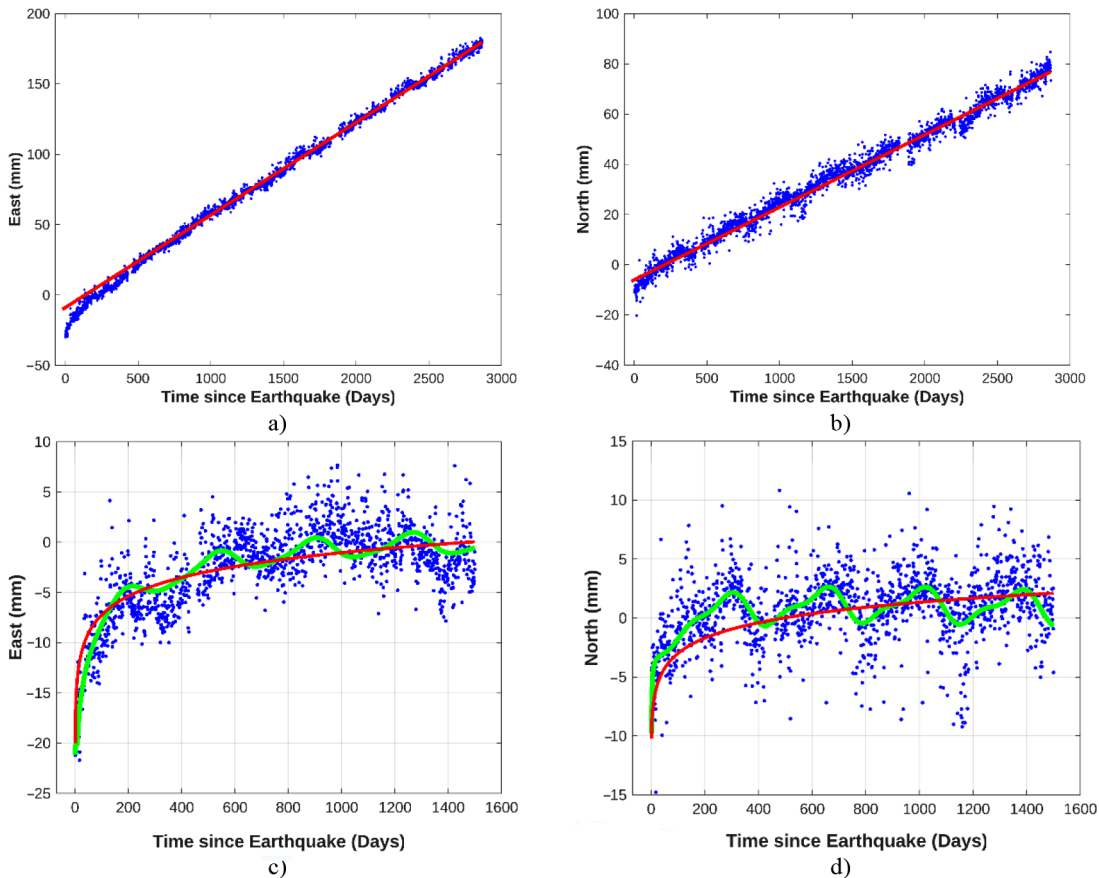


Figure 7. Time-series of local coordinates of station 018B in Samothrace after the earthquake: (a) and (b) show the East and North coordinates (blue dots) together with the straight line (in red) that represents the stable velocity of the station after the PSD; (c) and (d) show the detrended East and North coordinates (blue dots) together with the modeled seasonal variations (in green) and the estimated logarithmic function (in red) that describes the PSD

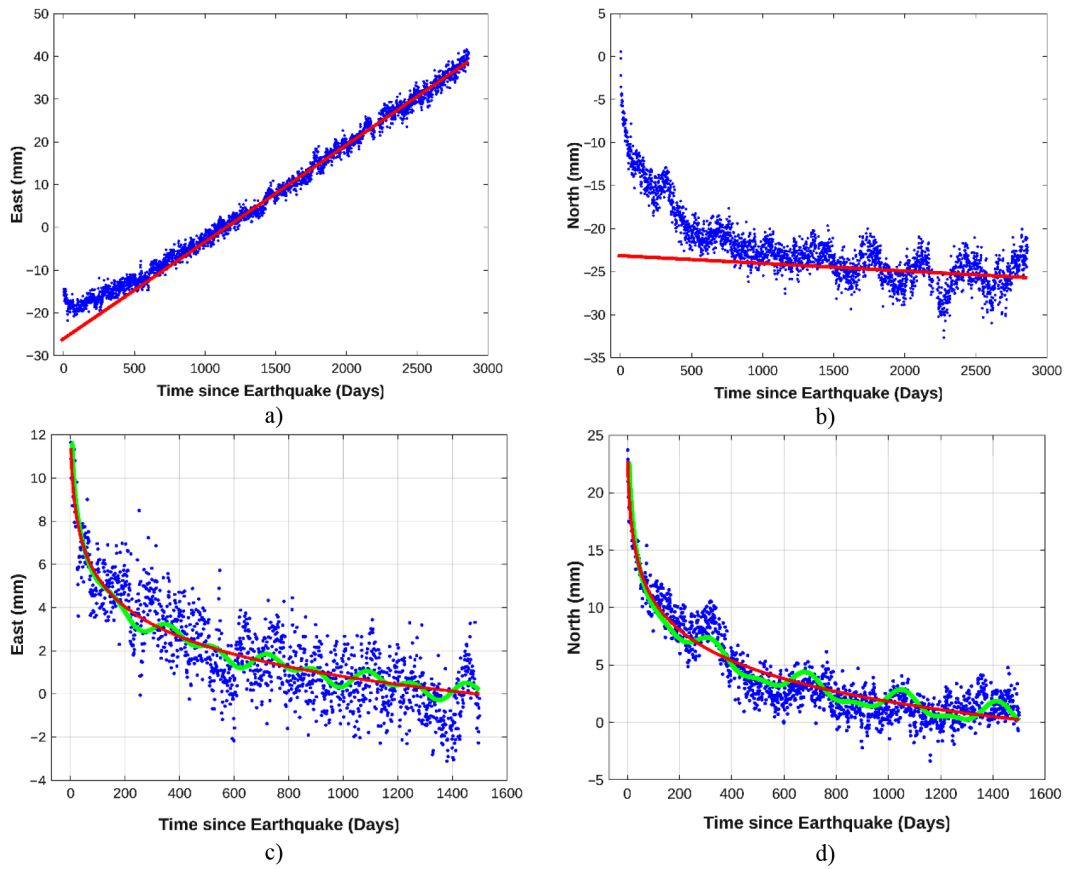


Figure 8. Time-series of local coordinates of station 089A in Lemnos after the earthquake (figure's structure and symbols are as in Figure 7)

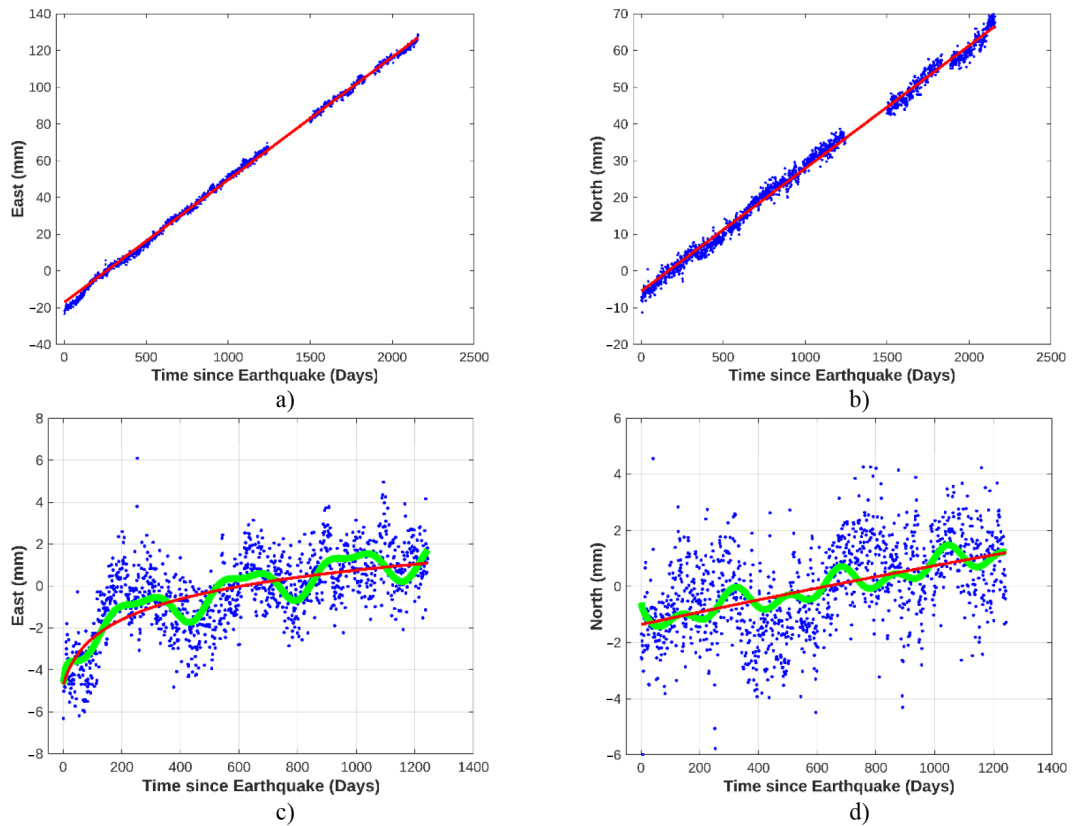


Figure 9. Time-series of local coordinates of station 019A near Alexandroupoli after the earthquake (figure's structure and symbols are as in Figure 7)

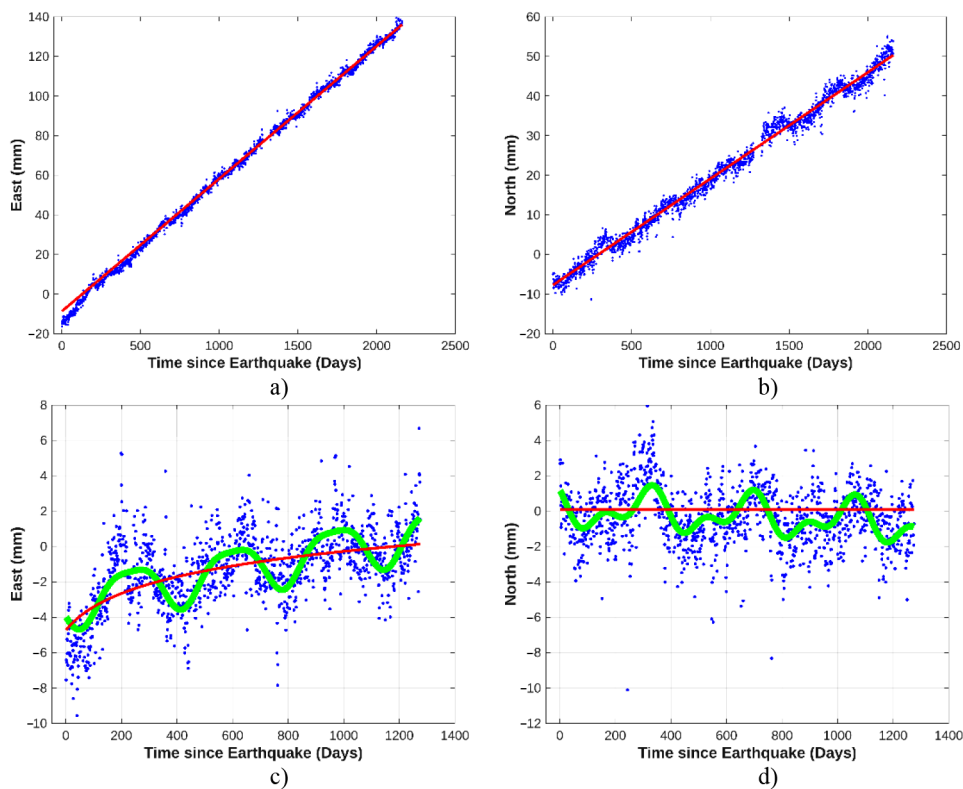


Figure 10. Time-series of local coordinates of station 036A in Thasos after the earthquake (figure's structure and symbols are as in Figure 7)

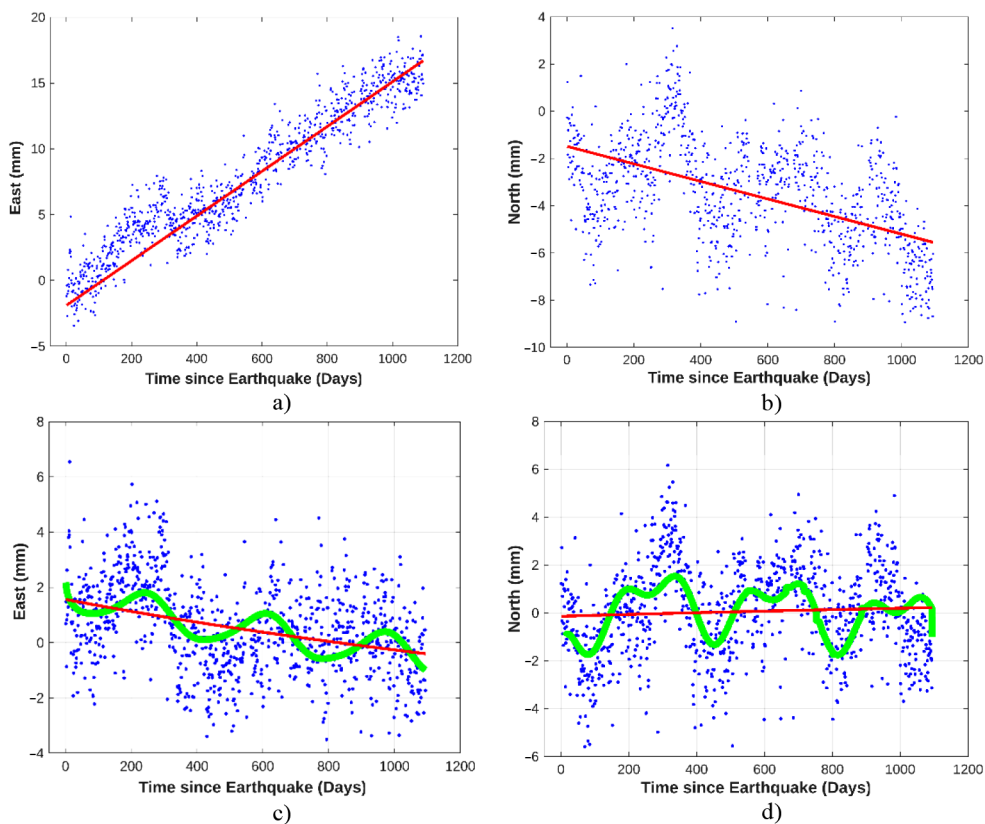


Figure 11. Time-series of local coordinates of station 091A in Lesbos after the earthquake (figure's structure and symbols are as in Figure 7)

displacements are estimated from the detrended coordinates' time-series, i.e. they describe a motion additional to the tectonic motion of each station. As shown in Table 2, the PSD in Samothrace affects more the East coordinate. On the contrary, in Lemnos the PSD affects mostly the North coordinate. This is in accordance with the directions and magnitudes of the co-seismic displacements of the stations (Saltogianni et al., 2015). This is shown in Figure 12, that depicts the co-seismic slip vectors together with the slip vectors describing the cumulative PSD.

Table 2. Cumulative PSD and decay times of the logarithmic functions describing the PSD at the stations used in the study

Station-Area	Cumulative PSD (mm)			Decay time (days)	
	East	North	2D	East	North
018B-Samothrace	-20±0.5	-10±0.4	22±0.5	2.8±0.9	2.4±1.8
089A-Lemnos	12±0.3	24±0.7	27±0.6	4.4±1.1	3.7±0.8
019A-Alexandroupoli	-5±0.2	-	-5±0.2	32±5.5	-
036A-Thasos	-5±0.2	-	-5±0.2	93±22.5	-
091A-Lesvos	-	-	-	-	-

### 2.2. Velocity changes

In order to search for changes in the stations' velocities, the stable velocities of the stations before and after the event were estimated and compared to each other. For estimating the velocities, we modeled the seasonal variations computing annual and semi-annual signals. Furthermore, we considered both white noise and colored

noise, as temporal correlated noise is well documented in GPS time-series (He et al., 2017). We estimated the unknown parameters and the parameters of the noise model by applying the Maximum Likelihood Estimation (MLE) using the HECTOR software package (Bos et al., 2013). We adopted a power law plus white noise model, after verifying that this combination represents our data well. One of the main advantages of modeling the temporal correlated noise in the GPS time-series is the estimation of realistic uncertainties for the velocities (Williams et al., 2004). For the time period 2008–2014.33 the stations' velocities are known to be stable (Gianniou & Stavropoulou, 2016); thus, all available data of 4-year duration (2010.33–2014.33) were used to estimate the velocities prior to the earthquake. However, as described in section 2.1, after the event the velocities were not constant as post-seismic motions took place lasting about three years (2014–2017) for the case of Samothrace and about four years (2014–2018) for the case of Lemnos. For these reasons, the stations' final velocities were estimated using the maximum available time period after the termination of the post-seismic motion at each station. In addition, each velocity was computed using a time period of integer multiples of years. In this way, the seasonal variations practically cancel out, ensuring results of high accuracy (Kenyeres & Bruyninx, 2004; Gianniou et al., 2019). Nevertheless, in order to achieve the highest possible accuracy, we modelled both annual and semi-annual signals before estimating the velocities. Concluding, for the velocity computation four years of data were used for stations 018B, 089A, 019A and 036A. Due to data limitation, two years of data were used for station 091A. The details about the used data can be found in Table 3.

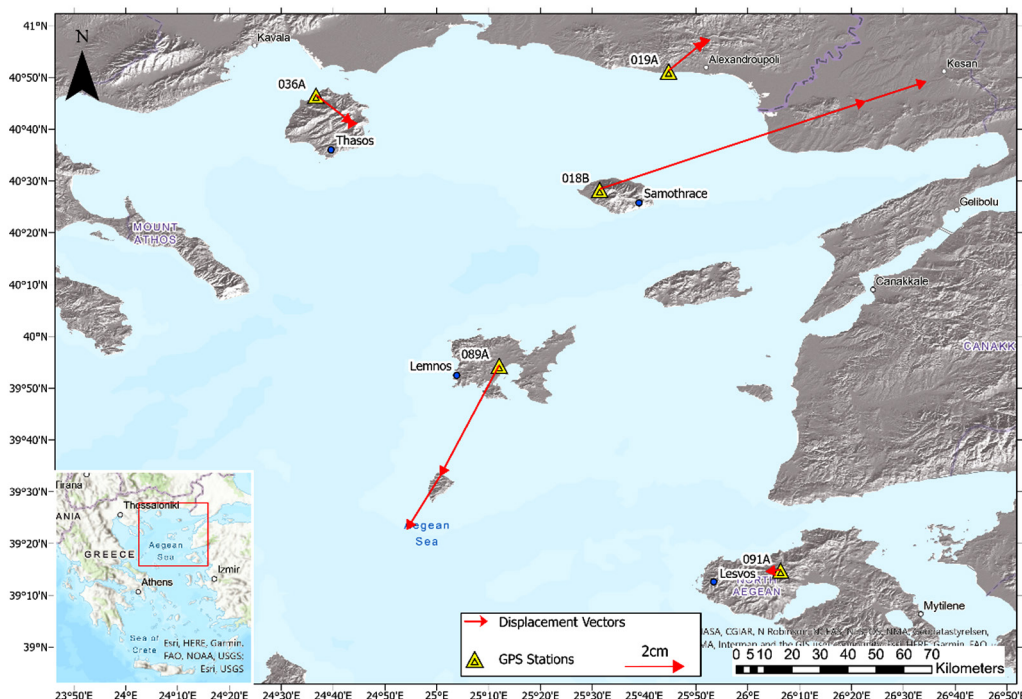


Figure 12. Co-seismic and post-seismic displacement vectors at the GPS stations

Table 3. Time periods used for the estimation of velocities after the termination of PSD

Station	Data available up to	Time period used for velocity estimation		Duration (years)
		Start	End	
018B	2022.33	2018.33	2022.33	4
089A	2022.33	2018.33	2022.33	4
019A	2020.33	2016.33	2020.33	4
036A	2020.33	2016.33	2020.33	4
091A	2017.33	2015.33	2017.33	2

The time-series used for the velocity estimations as well as the fitted trend lines for stations 018B and 089A are shown in Figures 13–14 (for the other stations these diagrams are omitted for the sake of brevity). The plots in these Figures are using the same range for the values in the X and the Y axes for each station. Thus, the slope of the fitted line before the earthquake can be compared to the slope after the earthquake. This helps visualize the changes in the kinematics of the stations due to the event. The estimated velocities are summarized in Table 4. The changes in the velocities are given in Table 5. As seen in Table 5, the horizontal velocities of stations 018B and 089A after the period of post-seismic deformation following the 2014 NAT earthquake are stabilized to values noticeably different than prior to the event. More precisely,

the velocity of station 018B in Samothrace increased by 1.8 mm/yr, whereas the velocity of station 089A in Lemnos decreased by 1.4 mm/yr. The velocity of station 019A near Alexandroupoli increased by 0.7 mm/yr. The change in the velocity of station 036A is smaller than its  $3\sigma$  confidence interval. The velocity change of station 091A cannot be considered reliable, as it is based on just two years of post-seismic data, a duration that does not ensure reliable velocity estimation (Legrand et al., 2021).

### 3. Discussion

It is known that strong earthquakes can be followed by PSD. The post-seismic deformation can occur as a result of a combination of processes, including viscoelastic relaxation of the upper mantle, afterslip on the fault plane including frictional afterslip, and poroelastic rebound (Golriz et al., 2021).

The analysis of the GPS data from the stations in the North Aegean Sea revealed that the 2014 NAT earthquake was associated by post-seismic motion. A first evidence of this post-seismic motion was given in previous studies which analyzed seven days of data after the earthquake and reported that the deformation evolved for two days after the event (Sboras et al., 2015; Bitharis et al., 2016). In this study we revealed a detailed pattern of the post-seismic deformation by analyzing data up to eight years after the earthquake. It is one of the few times, where PSD

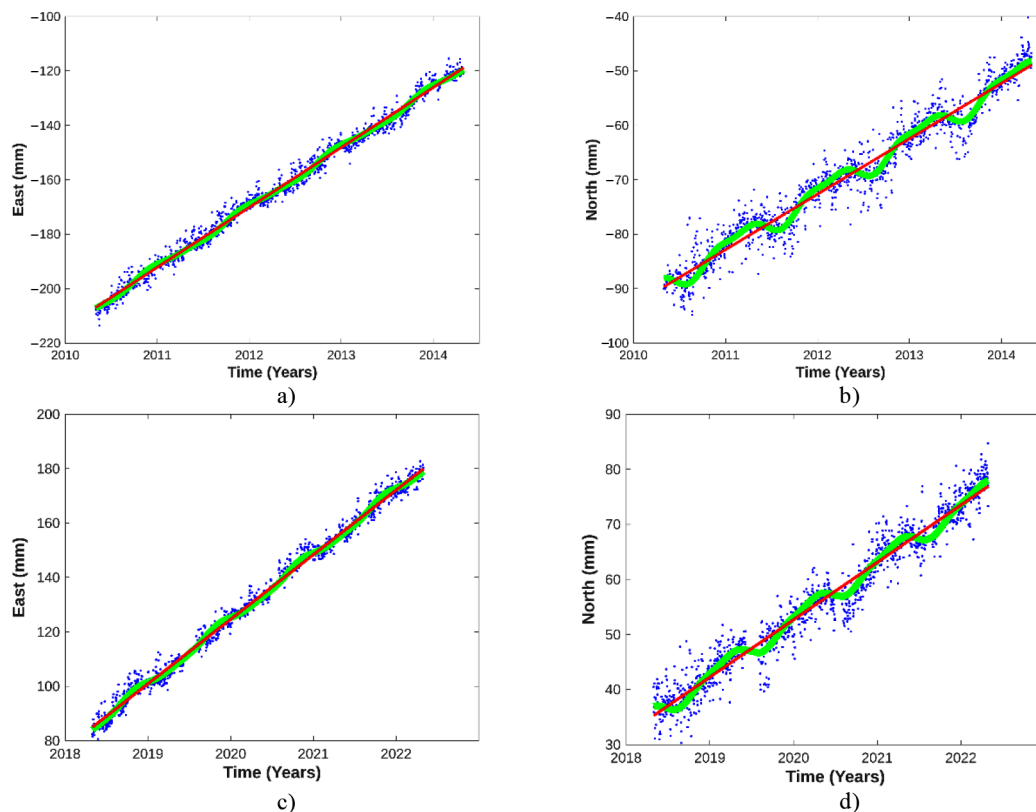


Figure 13. Time-series of local coordinates (blue dots) for station 018B in Samothrace: (a) East and (b) North coordinates before the earthquake; (c) East and (d) North coordinates after the earthquake. Straight lines (in red) represent the estimated velocities

is precisely estimated by GNSS and reported for an earthquake in Greece. Other events with documented PSD are the normal-fault 2020 Mw = 7.0 Samos earthquake (Ganas et al., 2021), the 2018 Mw = 6.7 Zakynthos earthquake (Ganas et al., 2020) and the 2014–2015 earthquakes in the Ionian Sea along the Cephalonia-Lefkada Transform Fault Zone (Sakkas et al., 2022).

The analysis of the post-seismic deformation and the estimation of logarithmic functions that describe this motion allowed the precise estimation of the cumulative PSD deformation at each station (Table 2). The post-seismic displacement vectors were compared with the co-seismic vectors, as shown in Figure 12. More specifically, the station in Lemnos showed a motion towards S22°W due to

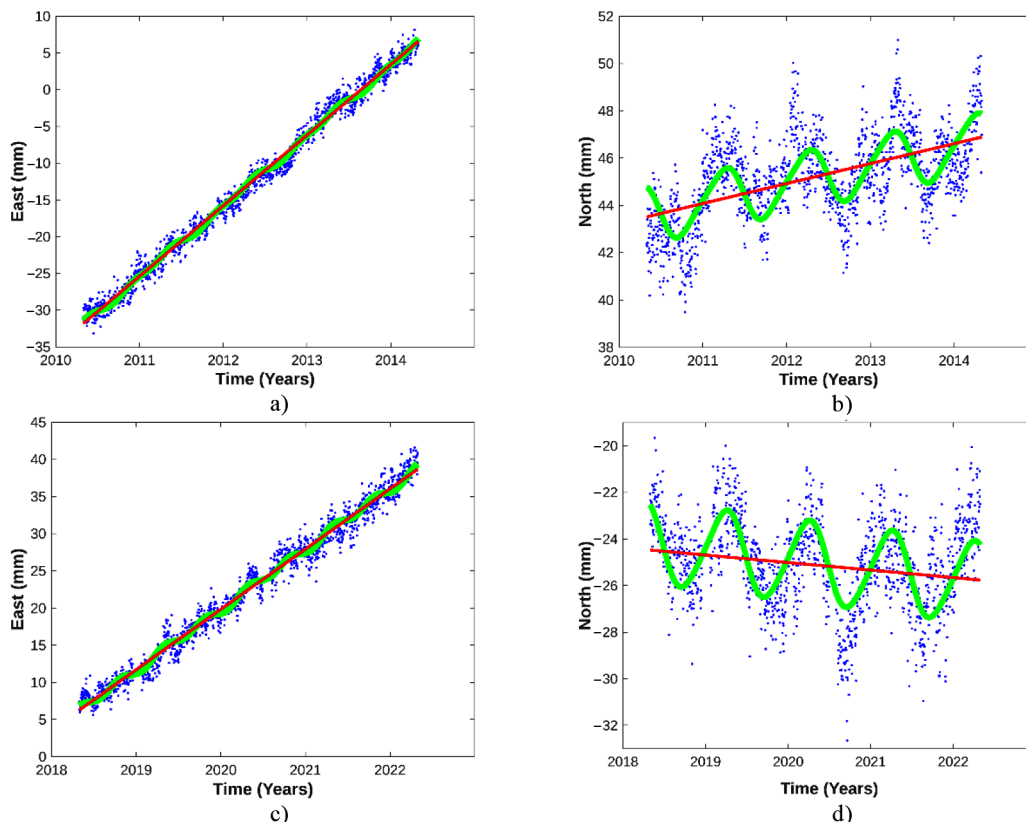


Figure 14. Time-series of local coordinates (blue dots) for station 089A in Lemnos: (a) East and (b) North coordinates before the earthquake; (c) East and (d) North coordinates after the earthquake. Straight lines (in red) represent the estimated velocities

Table 4. Estimates of stations' velocities (E, N) before and after the earthquake

Station	Velocity E (m/yr)		Velocity N (m/yr)	
	Before	After	Before	After
018B	0.0219±0.1E-3	0.0238±0.1E-3	0.0100±0.1E-3	0.0102±0.1E-3
089A	0.0095±0.1E-3	0.0081±0.1E-3	0.0009±0.2E-3	-0.0004 0.2E-3
019A	0.0233±0.1E-3	0.0240±0.1E-3	0.0115±0.2E-3	0.0117±0.1E-3
036A	0.0241±0.1E-3	0.0244±0.1E-3	0.0100±0.1E-3	0.0099±0.1E-3
091A	0.0054±0.1E-3	0.0061±0.1E-3	-0.0009±0.1E-3	-0.0019±0.4E-3

Table 5. Estimates of 2D stations' velocities before and after the earthquake along with the corresponding changes

Station	2D Velocity (m/yr)		2D Velocity Change (m/yr)
	Before EQ	Current	
018B	0.0241±0.1E-3	0.0259±0.1E-3	0.0018±0.1E-3
089A	0.0095±0.1E-3	0.0081±0.1E-3	-0.0014±0.1E-3
019A	0.0260±0.1E-3	0.0267±0.1E-3	0.0007±0.2E-3
036A	0.0261±0.1E-3	0.0263±0.1E-3	0.0002±0.1E-3
091A	0.0055±0.1E-3	0.0064±0.2E-3	0.0009±0.2E-3

the co-seismic displacement, similar to the direction of the post-seismic motion which was S26°W. The directions of the co- and post-seismic vectors for the station in Samothrace were N66°E and N67°E, respectively. Thus, co- and post-seismic vectors' directions are relatively well aligned. The magnitudes of the post-seismic displacement vectors are significantly smaller than the magnitudes of the co-seismic ones. More precisely, for station 018B the length of the 2D post-seismic vector was 23% of the length of the co-seismic one. For station 089A, the corresponding value was 49%. For station 019A near Alexandroupoli and station 036A in Thasos the PSD was very small (5 mm). This indicates that these stations are close to the northern boundaries of the area affected by PSD. The station 091A in Lesvos was not affected at all by PSD, which can be explained by its longer distance from the ruptured fault.

The analysis of the GPS data revealed that after the PSD period which followed the 2014 NAT earthquake, the 2D velocity of stations 018B and 089A was stabilized at a value that differs up to ~2 mm/yr compared to the velocity prior to the earthquake. This result refines the initial finding of Gianniou et al. (2017) who reported a velocity change of 5 mm/yr for station 089A. The difference between the two velocity estimations (2 mm/yr vs. 5 mm/yr) can be attributed to the fact that Gianniou et al. (2017) had assessed an approximate velocity using just two daily solutions per month which was not sufficient to reveal the PSD. Thus, their velocity included also the undetected PSD, leading to the overestimated value of 5 mm/yr. The velocity of station 091A in Lesvos appeared to be increased by ~1 mm/yr. However, this outcome should be treated with caution, as the available data after the event for this station are insufficient for reliable velocity estimation.

Velocity changes after seismic events have been reported also by other researchers that studied other strong earthquakes in Greece (e.g. Sakkas et al., 2022). Nevertheless, the number of studies that report velocity changes in Greece is quite limited. Thus, any new case of velocity change can significantly contribute to the knowledge of the tectonic settings in a certain area.

We believe that the investigation of the post-seismic kinematics of NAT should be continued in the future in order to estimate more precisely the velocities and monitor their long-term evolution.

## Conclusions

In this study, we analyzed twelve years of observations collected at five permanent GPS stations located around the epicenter of the 2014 North Aegean Sea earthquake. The analysis showed for the first time that this strong strike-slip earthquake caused post-seismic deformations lasting up to four years after the event. Based on other studies, GPS stations located in Turkey further away from the epicenter were not affected by PSD. Moreover, to the best of our knowledge, this is the first time that PSD is precisely documented along the North Aegean Trough by the use

of GPS data. The post-seismic vectors for the stations in Samothrace and Lemnos were found to be practically aligned to the co-seismic ones. Their magnitude ranged between 23% and 49% of the magnitude of the co-seismic vectors.

The 2014 North Aegean Sea earthquake also caused velocity changes in the area. After the time period of the PSD, the stations in Samothrace and Lemnos returned to a state of stable velocities which are up to 2 mm/yr different than the pre-seismic ones.

To summarize, according to our results, the 2014 North Aegean Sea earthquake considerably affected the NAT area's kinematics in terms of both PSD and velocity changes, findings that are in accordance with the characteristics of the NAT fault mechanism. The knowledge of these effects is important not only for understanding the tectonic settings of NAT, but also for operating the national RTK-network HEPOS.

## Acknowledgements

We are grateful to the Jet Propulsion Laboratory (NASA/JPL) and the California Institute of Technology for granting license to a binary version of the GipsyX software. The JPL is further-more acknowledged for the GNSS products used for the data processing. Part of the data of the Hellenic Positioning System's (HEPOS) that were used in this research were kindly provided free of charge by the Hellenic Cadastre to the Department of Surveying and Geoinformatics Engineering of UNIWA for supporting the Diploma Thesis of Mrs. T. Prasinou. The Department of Surveying and Geoinformatics Engineering and Mrs. Prasinou are grateful to the Hellenic Cadastre. Seismicity data were obtained from the National Observatory of Athens. Fault locations were retrieved from the GreDaSS and GEM GAF-DB databases.

## Author contributions

MG conceived the study and was responsible for the design and development of the data analysis. PA was responsible for the software automation and workflow optimization. MG, PA and TP were responsible for data collection and analysis. MG and PA were responsible for data interpretation. MG prepared the first draft of the article.

## Disclosure statement

The authors declare that have no competing financial, professional, or personal interests from other parties.

## References

- Altamimi, Z., Rebischung, P., Métivier, L., & Collilieux, X. (2016). ITRF2014: A new release of the international terrestrial reference frame modeling nonlinear station motions. *Journal of Geophysical Research: Solid Earth*, 121(8), 6109–6131. <https://doi.org/10.1002/2016JB013098>

- Bertiger, W., Bar-Sever, Y., Dorsey, A., Haines, B., Harvey, N., Hemberger, D., Heflin, M., Lu, W., Miller, M., Moore, A. W., & Murphy, D. (2020). GipsyX/RTGx, a new tool set for space geodetic operations and research. *Advances in Space Research*, 66(3), 469–489. <https://doi.org/10.1016/j.asr.2020.04.015>
- Bitharis, S., Fotiou, A., Pikridas, C., Rossikopoulos, D., Pavlides, S., & Chatzipetros, A. (2016). The Samothrace earthquake of May 2014 and the displacements estimations using permanent GPS stations data. *Bulletin of the Geological Society of Greece*, 50(3), 1545–1552. <https://doi.org/10.12681/bgs.11867>
- Boehm, J., Niell, A., Tregoning, P., & Schuh, H. (2006). Global Mapping Function (GMF): A new empirical mapping function based on numerical weather model data. *Geophysical Research Letters*, 33, L07304. <https://doi.org/10.1029/2005GL025546>
- Bos, M. S., Fernandes, R. M. S., Williams, S. D. P., & Bastos, L. (2013). Fast error analysis of continuous GNSS observations with missing data. *Journal of Geodesy*, 87, 351–360. <https://doi.org/10.1007/s00190-012-0605-0>
- Bulut, F. (2015). Different phases of the earthquake cycle captured by seismicity along the North Anatolian Fault. *Geophysical Research Letters*, 42, 2219–2227. <https://doi.org/10.1002/2015GL063721>
- Bulut, F., Özener, H., Dođru, A., Aktuđ, B., & Yaltrak, C. (2018). Structural setting along the Western North Anatolian Fault and its influence on the 2014 North Aegean Earthquake (Mw 6.9). *Tectonophysics*, 745, 382–394. <https://doi.org/10.1016/j.tecto.2018.07.006>
- Caputo, R., Chatzipetros, A., Pavlides, S., & Sboras, S. (2012). The Greek Database of Seismogenic Sources (GreDaSS): State-of-the-art for northern Greece. *Annals of Geophysics*, 55(5), 859–894. <https://doi.org/10.4401/ag-5168>
- Chousianitis, K., Ganas, A., & Evangelidis, C. P. (2015). Strain and rotation rate patterns of mainland Greece from continuous GPS data and comparison between seismic and geodetic moment release. *Journal of Geophysical Research: Solid Earth*, 120(5), 3909–3931. <https://doi.org/10.1002/2014JB011762>
- Erdik, M., Pinar, A., Akkar, S., Zülfikar, C., Kalafat, D., Kekovalı, K., Özel, N. M., & Necmiođlu Ö. (2014). *Earthquake report of 24 May 2014 Northern Aegean Sea*. Bođaziçi Technical University, KOERI. [http://www.koeri.boun.edu.tr/sismo/2/wp-content/uploads/2014/05/KOERI\\_Press\\_Bulletin\\_NAN\\_EQ\\_24May2014\\_v7.pdf](http://www.koeri.boun.edu.tr/sismo/2/wp-content/uploads/2014/05/KOERI_Press_Bulletin_NAN_EQ_24May2014_v7.pdf)
- Ergintav, S., Reilinger, R. E., Çakmak, R., Floyd, M., Çakır, Z., Dođan, U., King, R. W., McClusky, S., & Özener, H. (2014). Istanbul's earthquake hot spots: Geodetic constraints on strain accumulation along faults in the Marmara seismic gap. *Geophysical Research Letters*, 41(16), 5783–5788. <https://doi.org/10.1002/2014GL060985>
- Evangelidis, C. P. (2015). Imaging supershear rupture for the 2014 Mw 6.9 Northern Aegean earthquake by backprojection of strong motion waveforms. *Geophysical Research Letters*, 42(2), 307–315. <https://doi.org/10.1002/2014GL062513>
- Ganas, A., Briole, P., Bozionelos, G., Barberopoulou, A., Elias, P., Tsironi, V., Valkaniotis, S., Moschou, A., & Mintourakis, I. (2020). The 25 October 2018 Mw = 6.7 Zakynthos earthquake (Ionian Sea, Greece): A low-angle fault model based on GNSS data, relocated seismicity, small tsunami and implications for the seismic hazard in the west Hellenic Arc. *Journal of Geodynamics*, 137, 101731. <https://doi.org/10.1016/j.jog.2020.101731>
- Ganas, A., Elias, P., Briole, P., Valkaniotis, S., Escartin, J., Tsironi, V., Karasante, I., & Kosma, C. (2021). Co-seismic and post-seismic deformation, field observations and fault model of the 30 October 2020 Mw = 7.0 Samos earthquake, Aegean Sea. *Acta Geophysica*, 69(3), 999–1024. <https://doi.org/10.1007/s11600-021-00599-1>
- Gianniu, M. (2008). HEPOS: Designing and implementing an RTK-network. *GEOInformatics: Magazine for Surveying, Mapping & GIS Professionals*, 11, 10–13. [https://www.hepos.gr/hepos/HEPOS\\_pub\\_2008b\\_en.pdf](https://www.hepos.gr/hepos/HEPOS_pub_2008b_en.pdf)
- Gianniu, M. (2009, May 27–30). National report of Greece to EUREF 2009. In *Proceedings of the EUREF 2009 Symposium* (pp. 1–6), Florence, Italy. <http://www.euref.eu/symposia/2009Florence/07-12-p-Greece.pdf>
- Gianniu, M., & Stavropoulou, I. (2016, May 25–27). Estimation of tectonic velocities using GPS Precise Point Positioning: The case of Hellenic RTK network HEPOS. In *Proceedings of the EUREF 2016 Symposium* (pp. 1–8), San Sebastian, Spain. <http://www.euref.eu/symposia/2016SanSebastian/04-04-p-Gianniu-Stavropoulou.pdf>
- Gianniu, M., Mitropoulou, E., & Mastoris, D. (2017, May 17–19). National report of Greece to EUREF 2017. In *Proceedings of the EUREF 2017 Symposium* (pp. 1–7), Wrocław, Poland. <http://www.euref.eu/symposia/2017Wroclaw/05-10-p-Greece.pdf>
- Gianniu, M., Mitropoulou, E., & Mastoris, D. (2019, May 15–17). On the role of the length of GPS time-series in the accuracy of tectonic velocities' estimation: Examples from the HEPOS network. In *Proceedings of the 4th Joint International Symposium on Deformation Monitoring (JISDM)* (pp. 1–8), Athens, Greece. [https://www.fig.net/resources/proceedings/2019/04\\_JISDM2019/49.pdf](https://www.fig.net/resources/proceedings/2019/04_JISDM2019/49.pdf)
- Golriz, D., Bock, Y., & Xu, X. (2021). Defining the coseismic phase of the crustal deformation cycle with seismogeodesy. *Journal of Geophysical Research: Solid Earth*, 126(10), e2021JB022002. <https://doi.org/10.1029/2021JB022002>
- Görgün, E., & Görgün, B. (2015). Seismicity of the 24 May 2014 Mw 7.0 Aegean Sea earthquake sequence along the North Aegean Trough. *Journal of Asian Earth Sciences*, 111, 459–469. <https://doi.org/10.1016/j.jseaes.2015.06.018>
- He, X., Montillet, J. P., Fernandes, R., Bos, M., Yu, K., Hua, X., & Jiang, W. (2017). Review of current GPS methodologies for producing accurate time series and their error sources. *Journal of Geodynamics*, 106, 12–29. <https://doi.org/10.1016/j.jog.2017.01.004>
- Héroux, P., & Kouba, J. (2001). GPS precise point positioning using IGS orbit products. *Physics and Chemistry of the Earth, Part A: Solid Earth and Geodesy*, 26(6–8), 573–578. [https://doi.org/10.1016/S1464-1895\(01\)00103-X](https://doi.org/10.1016/S1464-1895(01)00103-X)
- Kenyeres, A., & Bruyninx, C. (2004). EPN coordinate time series monitoring for reference frame maintenance. *GPS Solutions*, 8, 200–209. <https://doi.org/10.1007/s10029-004-0104-8>
- Kiratzı, A. (2002). Stress tensor inversions along the westernmost North Anatolian Fault Zone and its continuation into the North Aegean Sea. *Geophysical Journal International*, 151(2), 360–376. <https://doi.org/10.1046/j.1365-246X.2002.01753.x>
- Konstantinou, K. I. (2017). Accurate relocation of seismicity along the North Aegean Trough and its relation to active tectonics. *Tectonophysics*, 717, 372–382. <https://doi.org/10.1016/j.tecto.2017.08.021>
- Kreemer, C., Blewitt, G., & Maerten, F. (2006). Co-and postseismic deformation of the 28 March 2005 Nias Mw 8.7 earthquake from continuous GPS data. *Geophysical Research Letters*, 33(7), L07307. <https://doi.org/10.1029/2005GL025566>
- Légrand, J., Bruyninx, C., Altamimi, Z., Caporali, A., Kenyeres, A., & Lidberg, M. (2021). *Guidelines for EUREF densifications*. IAG Sub-Commission for the European Reference Frame. [https://epncb.oma.be/\\_documentation/guidelines/Guidelines\\_for\\_EUREF\\_Densifications.pdf](https://epncb.oma.be/_documentation/guidelines/Guidelines_for_EUREF_Densifications.pdf)

- Müller, M. D., Geiger, A., Kahle, H.-G., Veis, G., Billiris, H., Paradissis, D., & Felekis, S. (2013). Velocity and deformation fields in the North Aegean domain, Greece, and implications for fault kinematics, derived from GPS data 1993–2009. *Tectonophysics*, 597, 34–49. <https://doi.org/10.1016/j.tecto.2012.08.003>
- Ohta, Y., Miura, S., Iinuma, T., Tachibana, K., Matsushima, T., Takahashi, H., Sagiya, T., Ito, T., Miyazaki, S., Doke, R., Takeuchi, A., Miyao, K., Hirao, A., Maeda, T., Yamaguchi, T., Takeda, M., Iwakuni, M., Ochi, T., Meilano, I., & Hasegawa, A. (2008). Coseismic and postseismic deformation related to the 2007 Chuetsu-oki, Niigata Earthquake. *Earth Planets Space*, 60(11), 1081–1086. <https://doi.org/10.1186/BF03353140>
- Pavlidis, S. B., & Tranos, M. D. (1991). Structural characteristics of two strong earthquakes in the North Aegean: Ierissos (1932) and Agios Efstratios (1968). *Journal of Structural Geology*, 13(2), 205–214. [https://doi.org/10.1016/0191-8141\(91\)90067-S](https://doi.org/10.1016/0191-8141(91)90067-S)
- Perez, J. A. S., Monaco, J. F. G., & Chaves, J. C. (2003). Velocity field estimation using GPS precise point positioning: The South American plate case. *Journal of Global Positioning Systems*, 2(2), 90–99. <https://doi.org/10.5081/jgps.2.2.90>
- Press, W. H., Teukolsky, S. A., Vetterling, W. T., & Flannery, B. P. (1992). *Numerical recipes in C* (2nd ed.). Cambridge University Press.
- Sakkas, V., Kapetanidis, V., Kaviris, G., Spingos, I., Mavroulis, S., Diakakis, M., Alexopoulos, J. D., Kazantzidou-Firtinidou, D., Kassaras, I., Dilalos, S., Vassilakis, E., Kotsi, E., Tselentis, G., Lekkas, E., & Voulgaris, N. (2022). Seismological and ground deformation study of the Ionian Islands (W. Greece) during 2014–2018, a period of intense seismic activity. *Applied Sciences*, 12(5), 2331. <https://doi.org/10.3390/app12052331>
- Saltogianini, V., Gianniou, M., Taymaz, T., Yolsal-Çevikbilen, S., & Stiros, S. (2015). Fault slip source models for the 2014 Mw 6.9 Samothraki-Gökçeada earthquake (North Aegean trough) combining geodetic and seismological observations. *Journal of Geophysical Research: Solid Earth*, 120(12), 8610–8622. <https://doi.org/10.1002/2015JB012052>
- Saltogianini, V., Gianniou, M., Moschas, F., & Stiros, S. (2016). Pattern of dynamic displacements in a strike-slip earthquake. *Geophysical Research Letters*, 43(13), 6861–6868. <https://doi.org/10.1002/2016GL069507>
- Satirapod, C., Simons, W., Promthong, C., Yousamran, S., & Trisirisatayawong, I. (2007). Deformation of Thailand as detected by GPS measurements due to the December 26th, 2004 Mega-Thrust Earthquake. *Survey Review*, 39(304), 109–115. <https://doi.org/10.1179/003962607X165069>
- Satirapod, C., Simons, W. J., & Promthong, C. (2008). Monitoring deformation of Thai geodetic network due to the 2004 Sumatra-Andaman and 2005 Nias earthquakes by GPS. *Journal of Surveying Engineering*, 134(3), 83–88. [https://doi.org/10.1061/\(ASCE\)0733-9453\(2008\)134:3\(83\)](https://doi.org/10.1061/(ASCE)0733-9453(2008)134:3(83))
- Sboras, S., Chatzipetros, A., Pavlides, S., Fotiou, A., Pikridas C., & Bitharis S. (2015, April 19–24). The May 24, 2014 North Aegean Trough earth-quake: Stress change and displacement patterns. In *Proceedings of the 6th International INQUA Meeting on Paleoseismology, Active Tectonics and Archaeoseismology* (pp. 356–360), Pescina, Fucino Basin, Italy.
- Scherneck, H.-G., & Bos, M. S. (2002, February 4–7). Ocean tide and atmospheric loading. In *Proceedings of the IVS 2002 General Meeting* (pp. 205–214), Tsukuba, Japan. <https://ivscc.gsfc.nasa.gov/publications/gm2002/scherneck.pdf>
- Şengör, A. M. C., Tüysüz, O., İmren, C., Sakıncı, M., Eyidoğan, H., Görür, N., Pichon, X., & Rangin, C. (2005). The north Anatolian fault: A new look. *Annual Review of Earth and Planetary Science*, 33, 37–112. <https://doi.org/10.1146/annurev.earth.32.101802.120415>
- Straub, C., Kahle, H. G., & Schindler, C. (1997). GPS and geologic estimates of the tectonic activity in the Marmara Sea region, NW Anatolia. *Journal of Geophysical Research: Solid Earth*, 102(B12), 27587–27601. <https://doi.org/10.1029/97JB02563>
- Styron, R., & Pagani, M. (2020). The GEM global active faults database. *Earthquake Spectra*, 36(1\_suppl), 160–180. <https://doi.org/10.1177/8755293020944182>
- Taymaz, T., Jackson, J., & McKenzie D. (1991). Active tectonics of the north and central Aegean Sea. *Geophysical Journal International*, 106(2), 433–490. <https://doi.org/10.1111/j.1365-246X.1991.tb03906.x>
- Tiryakioglu, I., Yigit, C. O., Yavasoglu, H., Saka, M. H., & Alkan, R. M. (2017). The determination of interseismic, coseismic and post-seismic deformations caused by the Gökçeada-Samothraki earthquake (2014, Mw: 6.9) based on GNSS data. *Journal of African Earth Sciences*, 133, 86–94. <https://doi.org/10.1016/j.jafrearsci.2017.05.012>
- Vigny, C., Simons, W. J. F., Abu, S., Bamphenyu, R., Satirapod, C., Choosakul, N., Subarya, C., Socquet, A., Omar, K., Abidin, H. Z., & Ambrosius, B. A. C. (2005). Insight into the 2004 Sumatra-Andaman earthquake from GPS measurements in south-east Asia. *Nature*, 436(7048), 201–206. <https://doi.org/10.1038/nature03937>
- Williams, S. D., Bock, Y., Fang, P., Jamason, P., Nikolaidis, R. M., Prawirodirdjo, L., Miller, M., & Johnson, D. J. (2004). Error analysis of continuous GPS position time series. *Journal of Geophysical Research: Solid Earth*, 109(B3), B03412. <https://doi.org/10.1029/2003JB002741>
- Zumberge, J. F., Heflin, M. B., Jefferson, D. C., Watkins, M. M., & Webb, F. H. (1997). Precise point positioning for the efficient and robust analysis of GPS data from large networks. *Journal of Geophysical Research: Solid Earth*, 102(B3), 5005–5017. <https://doi.org/10.1029/96JB03860>